Study on the post-fire properties of concrete with recycled tyre polymer fibres

Jelčić Rukavina, Marija; Baričević, Ana; Serdar, Marijana; Grubor, Martina

Source / Izvornik: **Cement & concrete composites, 2021, 123**

Journal article, Published version
Rad u časopisu, Objavljena verzija rada (izdavačev PDF)

https://doi.org/10.1016/j.cemconcomp.2021.104184

Permanent link / Trajna poveznica: https://urn.nsk.hr/urn:nbn:hr:237:767398

Cement and Concrete Composites 123 (2021) 104184

Contents lists available at ScienceDirect

Cement and Concrete Composites

journal homepage: www.elsevier.com/locate/cemconcomp

Study on the post-fire properties of concrete with recycled tyre polymer fibres

Marija Jelcic Rukavina *, Ana Baricevic, Marijana Serdar, Martina Grubor

University of Zagreb Faculty of Civil Engineering, Department of Materials, Fra Andrije Kacica Miosica 26, 10 000, Zagreb, Croatia

ARTICLE INFO

Keywords:
Fibre reinforced concrete
Post-fire properties
Recycled tyre polymer fibres (RTPF)
Polypropylene fibres (PPF)

ABSTRACT

This paper presents the results of an experimental study conducted to evaluate the effect of recycled tyre polymer fibres (RTPF) on the mechanical and durability properties of concrete after high temperature exposure. RTPF were used as an alternative to the commonly used polypropylene fibres (PPF) in concrete. Therefore, five different concrete mixes were tested: plain concrete, four mixes with 1 and 2 kg/m^3 of RTPF and PPF, respectively. The specimens were tested under ambient conditions and after exposure to a predefined elevated temperature of up to 500 °C, considering the fibre decomposition temperatures determined by the DTA/TG analysis. The results showed that when RTPF was used in concrete up to 2 kg/m^3, high temperatures did not cause further deterioration of the mechanical and durability properties of concrete due to their melting. On the contrary, certain benefits of RTPF were found compared to PPF, possibly due to the higher amount of residue at high temperatures.

1. Introduction

Decades of research have shown that although the behaviour of concrete at high temperatures is relatively favourable compared to other building materials (particularly due to its inorganic and noncombustible nature), exposure to elevated temperatures leads to various physical, chemical and mechanical processes [1,2]. These processes can negatively affect the mechanical concrete properties and cause explosive spalling of the reinforcement protection layer ultimately leading to a reduction in the load-bearing capacity of the reinforced concrete structure. Explosive spalling of concrete results in the breaking up of layers/pieces of concrete from surface exposing reinforcement to rising temperature. The risk of its occurrence is governed by many factors, which include environmental (e.g. rate of heating), or factors related to concrete mix (concrete strength, moisture content, permeability, density, size and type of aggregates, etc.) [2,3]. Although explosive spalling has been regularly reported to occur within types of concrete with dense microstructure (high strength, reactive powder, self-compacting etc.) [4], an experimental study performed by Van der Waart van Gulik et al. [5] showed that explosive spalling can occur also in ordinary normal strength concrete under harsh heating regimes as defined by RWS fire exposure. Due to the complexity of the phenomenon, which takes into account the interaction between hygro-thermal and mechanical behaviour of concrete at high temperatures, to date there is no generally accepted mechanism for the occurrence of explosive spalling. In the available literature, mainly two theories have been proposed for the explanations for the occurrence of explosive spalling which are: 1) pressure build-up in the concrete pores as a result of physically/chemically bound water [6–9] and 2) thermal stresses near the heated surface due to pre-stress or a high temperature gradient caused by a high heating rate [10–12]. Liu et al. [13] recently proposed three types of fire-induced concrete spalling depending on the three spalling mechanisms, i.e., thermo-hygral spalling which corresponds to the first earlier mentioned theory, thermo-mechanical spalling corresponding to the second one and additional third type which is thermo-chemical spalling. This type of spalling can be further divided into sloughing-off spalling occurring at extreme high temperatures and post-cooling spalling occurring after exposure to fire. Furthermore, due to complexity of mechanism of occurrence, standard procedures for testing the explosive spalling are also lacking so far.

The most widely used technological solution to prevent concrete spalling is the addition of low melting point fibers such as polypropylene fibers (PPF), which has been well documented in both scientific and technical literature to date [4,9,14–17]. EUROCODE 2 [18] suggests only the amount of PPF (2 kg/m^3) without specifying the required dimensions. However, studies in this field have shown that the PPF

* Corresponding author.
E-mail address: marija.jelcic.rukavina@grad.unizg.hr (M. Jelcic Rukavina).

https://doi.org/10.1016/j.cemconcomp.2021.104184
Received 16 April 2021; Received in revised form 5 July 2021; Accepted 14 July 2021
Available online 17 July 2021

content in concrete needed to reduce the risk of explosive spalling is usually between 1 and 3 kg/m^3 of concrete, depending on several factors, the most important being the severity of the fire, the moisture content in the concrete, the permeability of the concrete and the dimensions of the PPF [14,19]. For example, Bilodeau et al. [20] reported that in lightweight concrete with low w/c ratio and silica fume exposed to hydrocarbon fire, 3.5 kg of 20 mm or 1.5 kg of finer but shorter (12.5 mm) PPF per m^3 was sufficient to prevent explosive spalling.

When heated, PPF melt at temperatures of around 160–170 °C and evaporate at a temperature of about 340 °C [14,15]. Four different mechanism are recognized according to which PPF mitigate explosive spalling in concrete material, i.e. (1) increased permeability due to formation of capillary pores upon fibres melting [9,21], (2) increased connectivity between the interfacial transition zone (ITZ) [16], (3) development of additional air pores during concrete mixing [22] and (4) development of additional microcracks at the tips of the fibre beds during heating [23]. Due to the low volumetric content in concrete, these fibres do not have a significant effect on the mechanical and physical properties of concrete at room temperature [4,9,24] but they positively affecting on reducing early age deformation, autogenous and plastic shrinkage [25–28]. In addition, PPF improve permeability properties [29,30], resistance to chloride diffusion [30] and reduce concrete degradation due to freeze-thaw cycles [31].

However, the production of PPF leads to increased carbon dioxide emissions [32] and its replacement by waste materials in concrete will certainly contribute to the greening of the construction industry. Waste tyres consist of approximately 80% rubber granules reinforced with 15% steel and 5% polymer fibre reinforcement [33,34]. Compared to other waste tyre components, the reusability and storage of recycled tyre polymer fibres (RTPF) has been limited as the material is combustible and easily carried away by wind.

Previous studies have shown that RTPF can be used as a PPF replacement to reduce early age deformations in various types of cement composites [33–38] and restrained shrinkage [33,35]. Moreover, RTPF improved the behaviour of concrete when exposed to aggressive environments [33,34] as well as the mechanical behaviour under high strain rate and cyclic loading [39,40]. Furthermore, the results of studies in Refs. [41–43] showed that the addition of RTPF to the concrete mix in an amount equal to or exceeding 2 kg/m^3 has the potential to prevent spalling of high-strength concrete (HSC) during exposure to ISO or hydrocarbon fire. Regarding the effect of RTPF on the mechanical and durability properties of concrete at high fire temperatures, only Santos et al. [44] investigated the compressive strength of concrete with 2 and 4 kg/m^3 of RTPF during exposure (hot state properties) to high temperatures of 700 °C and compared it with conventional concrete without the fibres. The study showed that at temperatures above 500 °C, both mixes with RTPF gave about 20% better results compared to the reference mix, while in the lower temperature range, only the mix with the lower amount (2 kg/m^3) gave better results. However, the literature review shows that other properties of concrete with RTPF after high temperature exposure (post-fire properties) have not been studied so far.

In this regard, the aim of the study was to evaluate the behaviour of concrete with addition of RTPF after high temperature exposure for use in fire aggressive environment. For this purpose, the behaviour of RTPF was first analysed using DTA/TG to understand the changes that the material undergoes at different temperatures. Therefore, critical temperatures at which changes in the material occur were noted. Next, microscopic behaviour of fibres during heating at the same temperatures was documented in real time using a polarizing microscope with a temperature-controlled stage compartment. SEM analysis was used to observe the condition of the fibres in the heated concrete. Finally, the post-fire properties of concretes with up to 2 kg/m^3 of RTPF were determined in terms of compressive strength, modulus of elasticity, capillary absorption and ultrasonic pulse velocity. The obtained results were compared with those of conventional concrete and concrete with the same dosage of PPF.

2. Materials and methods

2.1. Microfibers

Two types of polymer microfibers were used for this study: commercial monofilament PPF and RTPF as presented in Fig. 1. The RTPF sample, which was supplied by Croatian tyre recycling company Gumiimpex GRP, contained more than 65% rubber particles. Therefore, a cleaning procedure based on a previous study [34] was used to remove most of the rubber particles from the fibres. The composition of cleaned RTPF is 60% polyester poly (ethylene terephthalate) - PET, 25% polyamide 66 - PA66, and 15% poly (butylene terephthalate) - PBT with a small amount of tiny rubber particles attached to the fibres [34]. The length distribution ranges from 8 to 38 mm, but the average length is 9.5 ± 4.6 mm and more than 80% of the fibres have a length of less than 13 mm. The properties of the used fibres are presented in Table 1, where properties of PPF were declared by the producer.

Fig. 2 shows a SEM micrograph of a PPF that has a smooth surface, a flat shape, and a circular cross-section. Fig. 3 shows a SEM micrograph of a typical RTPF bundle, which consists of fine, slightly curved fibres with a mostly circular cross-section. The surface of most of the fibres in the bundle is rough, which may provide improved adhesion at the fibre/matrix interface compared to PPF.

2.2. Concrete mix design

All studied concrete mixes contained crushed limestone aggregate, from the Zvečaj quarry in Croatia, with maximum grain size of 16 mm (fractions corresponding to 0/4, 4/8 and 8/16 mm) and particle-size distribution determined according to HRN EN 933–1 [45] as shown in Fig. 4.

The cement used was CEM II/BM SV 42.5 N, in accordance to HRN EN 197–1 [46]. The water used was from the general city drinking-water supply which contained a negligible amount of chloride substances. Polycarboxylic ether hyperplasticizer was added during concrete production to obtain target workability.

Table 2 shows the proportions of constituents in the mixes studied and the results in the fresh state. The absolute volume method was used to design the concrete mixes keeping the water-cement ratio constant at 0.46 with 370 kg/m^3 cement and 170 l/m^3 water. Superplasticizer was added during mixing of concrete to achieve consistency class S4 (160–210 mm). The study included the following concrete mixes:

- reference mix of plain concrete (referred to as PC in Table 2)
- two mixes containing 1 and 2 kg of monofilament PPF per m^3 of concrete (referred to as 1PPF and 2PPF respectively in Table 2)
- two mixes containing 1 and 2 kg of cleaned RTPF per m^3 of concrete (referred to as 1RTPF and 2RTPF respectively in Table 2).

2.3. Concrete production and curing

All materials were stored in the laboratory at a temperature of 20 ± 2 °C for 24 h before mixing. The concrete was mixed in a laboratory mixer with a maximum volume of 60 L. For mixes that contained fibres, the aggregates and fibres were first mixed together to ensure good dispersion of the fibres. Then mixing was done for 2 min after adding half of the water. Mixing was stopped for about 2 min to allow the aggregates to absorb the required amount of water. The cement was then added and mixing continued with the continuous addition of residual water and superplasticizer. After all the materials were added to the concrete mixer, mixing was continued for another 2 min. The concrete was compacted on a vibrating table at a frequency of 150 Hz. The fresh concrete properties (shown in Table 1) were determined immediately after mixing. After casting into moulds, the test specimens were kept covered under laboratory conditions for 24 h until demoulding to prevent water evaporation. After demoulding, the test specimens were kept

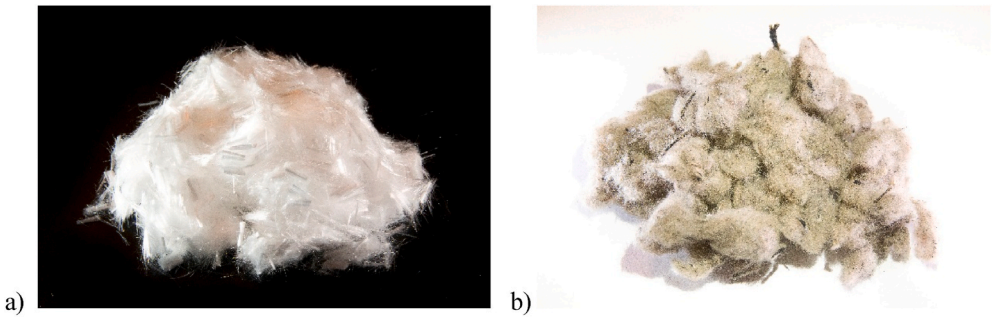

Fig. 1. Photo of the appearance of a) PPF and b) RTPF.

Table 1
Properties of microfibers [25,27].

Type of fibers	Average length (mm)	Diameter (μm)	Density (g/cm^3)
Polypropylene fibres (PPF)	6	approx. 32	0.91
Recycled tyre polymer fibres (RTPF)	9.5 ± 4.6	type 1 30.1 ± 2.0 type 2 20.2 ± 1.7 type 3 12.4 ± 1.8	1.32

in a mist room at 20 ± 2 °C and RH ≥ 95% until 28 days of age, and then left under normal laboratory conditions (20 ± 2 °C and RH ≈ 40–50%) in the laboratory of the Department of Materials of the University of Zagreb until the time of testing (more than 1 year).

Three types of specimens were prepared:

1. Cylindrical specimens with dimensions Ø = 75 mm and L = 225 mm (i.e. slenderness equal to 3). Although non-standard specimen dimensions were chosen, they are consistent with RILEM recommendations for high-temperature testing [47–49], which recommend a length-to-diameter (slenderness) ratio between 3 and 4 and a specimen diameter greater than 4 times the largest aggregate size (16 mm in this case).
2. Specimens for monitoring the microstructure (SEM analysis) before and after exposure to high temperature were prepared from the specimens described above.
3. Cylindrical specimens with dimensions Ø = 100 mm and L = 50 mm to determine residual capillary absorption of heated concrete.

2.4. Methods

2.4.1. Thermal behaviour of fibers

In this paper thermal behaviour of fibers was obtained by thermogravimetry (TG) and their microscopic behaviour under elevated temperatures. Thermal properties of the fibres were investigated using

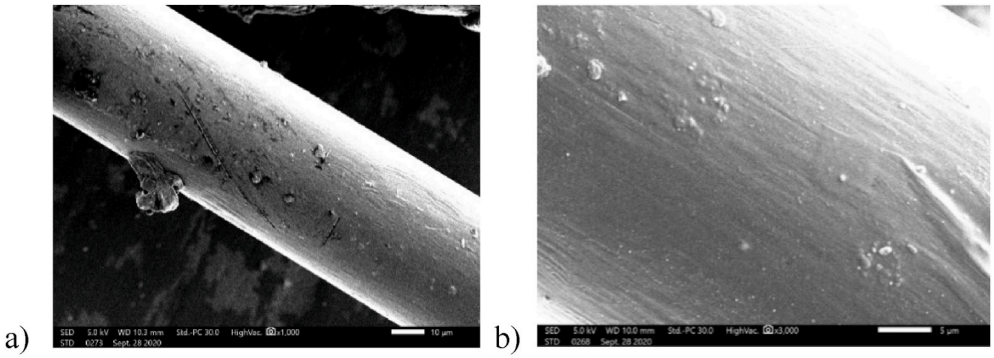

Fig. 2. SEM micrographs of the PPF a) 1000x b) 3000x

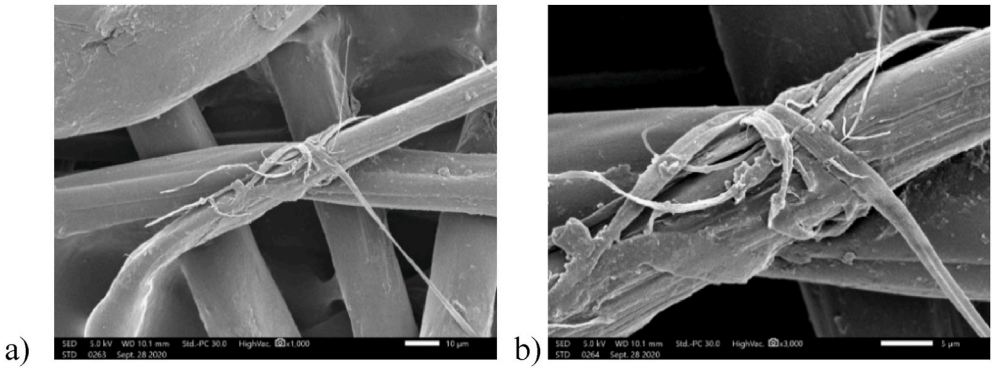

Fig. 3. SEM micrographs of the RTPF fibers a) 1000x b) 3000x

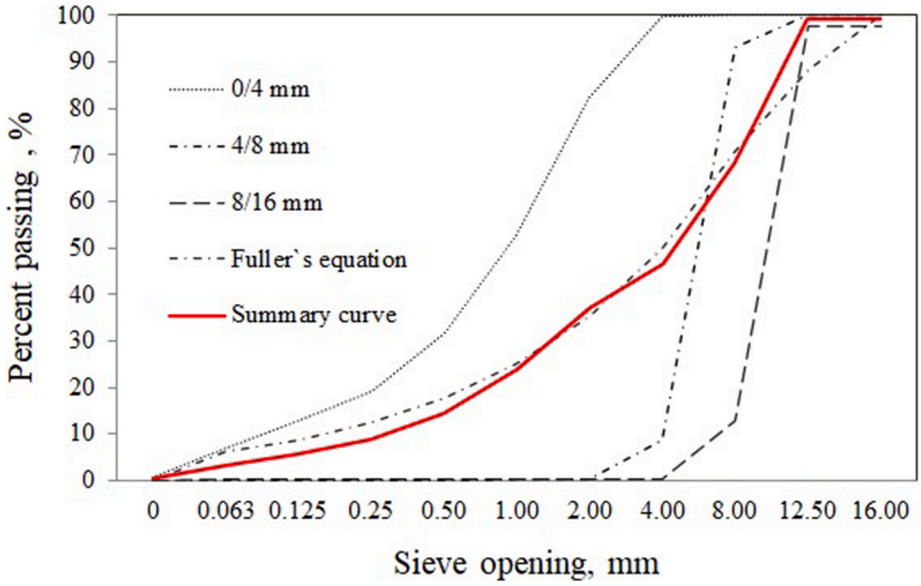

Fig. 4. Aggregate grading curves.

Table 2
Mix designs per m^3 of concrete.

Components, kg	PC	1PPF	2PPF	1RTPF	2RTPF
Cement			370		
Water			170		
W/C ratio			0.46		
Superplasticizer	2.2	2.05	1.70	1.29	1.67
PPF	–	1	2	–	–
RTPF	–	–	–	1	2
Aggregate 0/4 mm	899	880	878	880	878
Aggregate 4/8 mm	347	344	344	344	344
Aggregate 8/16 mm	590	603	602	603	602
Fresh concrete properties					
Mass per unit volume (kg/m^3)	2390	2389	2379	2385	2359
Air content (%)	1.5	2.2	2.3	1.9	3
Slump test (mm)	175	175	180	175	175

differential thermal analyser TG/DSC NETZSCH STA 409 PC LUXX. The samples (120 ± 0.1 mg) were tested at a constant heating rate of 10 °C/min up to 1150 °C under nitrogen flowrate (80 mL/min).

Microscopic behaviour of both used polymeric fibres during heating were followed by Nikon Aclipse LV150NL, a polarizing microscope with a stage compartment that is temperature controlled by a computer and a digital camera (Optoteam OPTOCAM II) with a resolution of 1600 × 1200 pixels. The microscope is equipped with a controller (Linkam T95-PE) used to control the temperature profile either manually or by means of an automated program to a temperature of 0.1 °C up to ~ 600 °C with a resolution of 0.01 °C.

2.4.2. *Thermal treatment of concrete specimens*

Temperature exposure followed the recommendations of RILEM recommendations for high-temperature testing [47]. The specimens were exposed to three different temperature cycles using an electric furnace (with T_{max} = 1400 °C).

The temperature cycle consisted of the following steps:

1. Heating at a rate ΔT/Δt of 2 °C/min to the maximum target temperature (200 °C, 300 °C and 500 °C).
2. Holding the target temperature until it was reached in the middle of the specimens (approximately 3 h).
3. Slowly cooling to ambient temperature within the closed furnace to avoid thermal shock and subsequent micro-cracking of the concrete material.

The slow temperature increase was chosen to avoid explosive spalling and high temperature gradients in the specimens, and thus severe microcracking, which would affect the experimental results. For each target temperature, seven specimens from the same mix were subjected to a temperature cycle (Fig. 5a), with one specimen used to monitor the temperature at its middle. For this purpose, a K-type thermocouple was placed in the center of the specimens before casting (Fig. 5b).

After cooling, the specimens were removed from the furnace and left at normal laboratory conditions (T = 20–25 °C; R.H. = 50–70%) until testing.

Explosive spalling did not occur during heating in any of the specimens used for this study. The absence of explosive spalling in the heated specimens can be explained by the low moisture content, since the heating was carried out when the specimens were more than an year old, and by the slow temperature rise of 2 °C/min in the furnace during temperature treatment. In addition, due to the relatively small dimensions of tested specimens, the risk of spalling is reduced because the residual moisture could easily evaporate resulting in a lower pore pressure.

2.4.3. *Residual properties of concrete*

The residual properties of the thermally treated specimens were determined 7 days after the specimens had cooled to room temperature, when the greatest decrease was expected according to Hertz [50], and the following testing methods were used:

- The morphology and microstructure of the concrete mixtures were analysed on polished specimens in the transverse direction in a JEOL 5500 LV SEM coupled with an Oxford energy dispersion spectrometer using backscattered electrons and a low vacuum. The analysis conditions were as follows: an accelerating voltage of 20 kV, a working distance of 20 mm and a working pressure of 10–20 Pa.
- Compressive strength was determined according to the RILEM recommendation for compressive strength testing at high temperatures [48], using a hydraulic Toni Technik testing machine with a capacity of 3000 kN and a velocity of the applied load of 0.5 MPa/s.
- The static modulus of elasticity was determined according to the RILEM recommendation for testing of residual modulus of elasticity

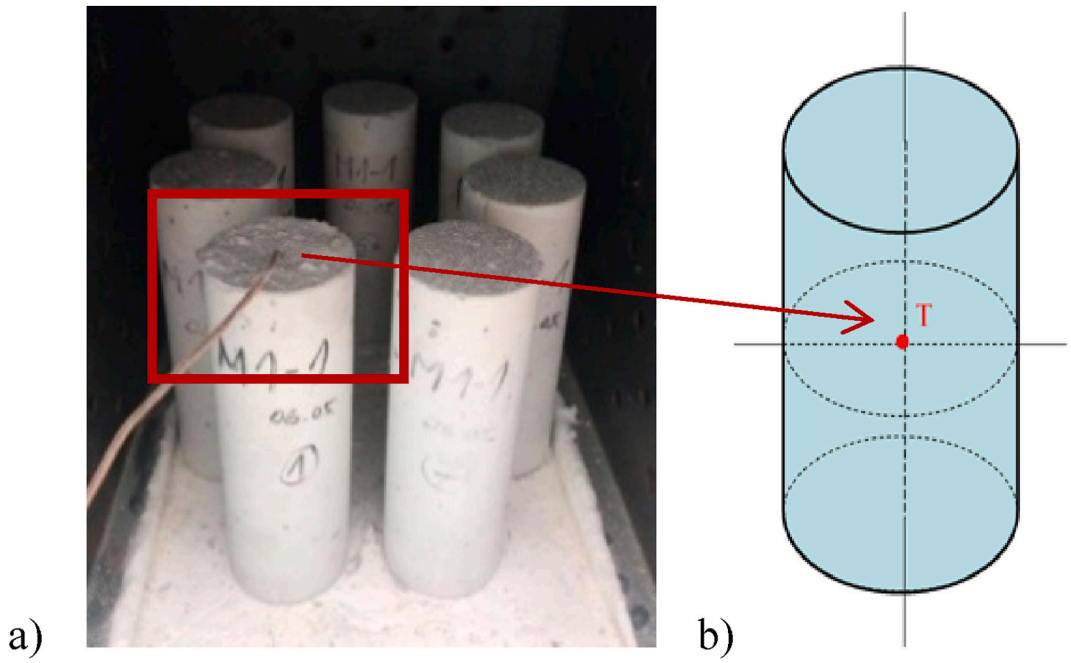

Fig. 5. a) Position of the specimens in the furnace during thermal treatment; b) Position of K-type thermocouple (T) in the center of cylindrical specimen.

after cooling [49] using the same equipment as for compressive strength.
- The capillary absorption test was performed according to HRN EN 13057 [51]. After recording the dry weight of each specimen, one side was partially immersed in water. The mass gain was recorded at fixed times, i.e. 0.2, 0.5, 1, 2, 4 and 24 h, respectively using precision balance of 0.001 g.
- Ultrasonic pulse velocity (UPV) was measured along the longitudinal direction of the cylinder according to HRN EN 12504–4 [52]. The tests were performed using a TICO Proceq UPV tester with transducers of 54 Hz.

To evaluate the effect of elevated temperatures on concrete properties, the same testing methods were used to test the unheated specimens from each tested mix.

3. Results and discussion

3.1. Thermal behaviour of microfibers

Differential thermal analysis, DTA (a), and thermogravimetric analysis, TGA (b) and derivative TG, dTG (c) of PPF and RTPF are presented in Fig. 6. The results are based upon testing of three specimens and hereafter an average of these three measurements is shown.

In the case of PPF, it can be observed from the DTA diagram that the glass transition of PPF fibres starts at 140 °C. At this temperature, there is a slight mass increase of up to 0.5% of the original fibre mass. At a temperature of 325 °C, the mass of PPF starts to decrease, indicating the decomposition of fibres, with a peak temperature of decomposition at 450 °C, where 50% of the mass is lost. After 500 °C, about 14% and after 600 °C about 12% of the residue remains.

As previously mentioned in this manuscript, RTPF consist of 60% PET, 25% PA 66 and 15% of PBT. From DTA diagram in Fig. 6a, two fusion peaks can be observed, one at around 225 °C and the other at 340 °C. Lower temperature peak arises from PBT melting and the higher temperature peak is probably due to simultaneous melting of both PET and PA 66. From TG and DTG diagrams, in Fig. 6b and c, it can be observed that the melting of a crystalline part of RTPF occurs at 225 °C, followed by a continuous mass loss. The decomposition of fibres occurs at two main peaks, one at around 340 °C (connected to full decomposition of PBT) and the other at 400 °C (connected to full decomposition of PET and PA 66). After 500 °C around 20% of residue is left.

Fig. 7 show melting of PPF, taken using a polarizing microscope with a temperature-controlled stage compartment.

Fig. 7a shows stable PPF at 51.8 °C, while Fig. 7b shows beginning of melting at 149.6 °C. Finally, melted fibre at 172 °C is shown in Fig. 7c. On the last image (Fig. 7c) the focus of the microscope changed, and the fibre is shown with higher magnification, compared to Fig. 7a and b. Still, it is visible that the fibre is melted, but not turned into vapour. The whole process of melting of both types of fibers can be seen in videos attached in appendix A of this manuscript.

Fig. 8 show melting of RTPF, taken using a polarizing microscope with a temperature-controlled stage compartment.

Fig. 8a shows stable RTPF at 149.6 °C, temperature at which PPF was already started to melt and increasing its mass. Fig. 8b shows beginning melting of RTPF at 302.9 °C. Finally, melted RTPF at 391.1 °C is shown in Fig. 8c, showing high volume of residue.

From thermal analysis and comparison between PPF and RTPF, it can be concluded that PPF start to melt at lower temperatures compared to RTPF, but their mass is initially increasing. RTPF start to melt at higher temperature of 225 °C, immediately experiencing loss in mass. PPF start losing their mass at 325 °C, with peak in their decomposition at 450 °C, which is higher temperatures compared to RTPF (395 °C). Finally, there is a higher leftover mass of unburned material in the case of RTPF (20% compared to 12% in the case of PPF), which is attributed to unburned rubber attached to RTPF.

In accordance to obtained results, the maximum target temperature in each thermal cycle was chosen to investigate the effect of decomposition of RTPF on the residual concrete properties after heating and to compare with the effect of PPF. Therefore, the maximum temperature for concrete specimens in each thermal cycle were chosen as follows:

- 200 °C – glass transition of PPF starts at 140 °C, while RTPF is still stable
- 300 °C – melting of crystalline part of RTPF starts at 225 °C
- 500 °C – both types of fibers mostly decomposed.

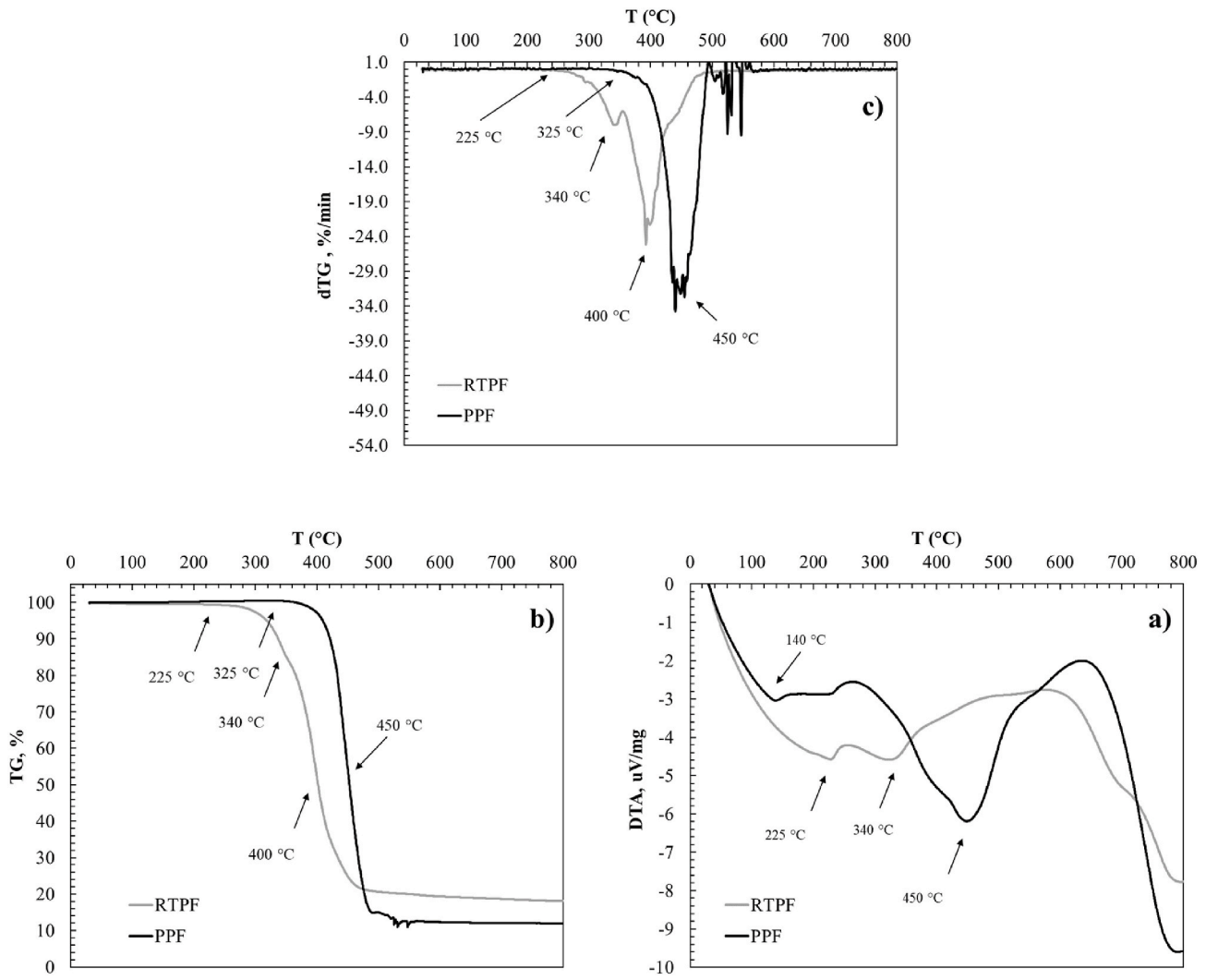

Fig. 6. a) Differential thermal analysis, DTA, b) thermogravimetric analysis, TGA and c) derivative of thermogravimetry (dTG) of PPF and RTPF.

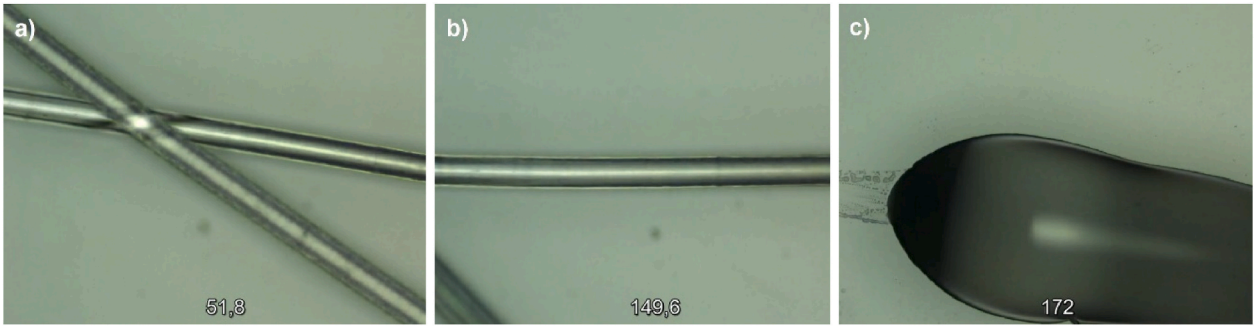

Fig. 7. a) Stable PPF (image taken at 51.8 °C), b) PPF starting to melt (image taken at 149.6 °C), and c) melted PPF increasing in volume (image taken at 172.6 °C).

3.1.1. Decomposition of fibres in concrete

SEM images of concrete with PPF and RTPF after exposure to temperatures 200 °C and 500 °C are shown in Fig. 9. After heating to 200 °C, the PPF decomposed in their initial channel, while RTPF had not yet started to decompose. The decomposed PPF are absorbed by the cement matrix.

Moreover, some micro-cracks are observed around empty channels, which is in agreement with the observations of Kalifa et al. [9], who concluded that these cracking around fibres has the positive effect of reducing the water vapour pressure, helping to prevent explosive spalling in the concrete. Nevertheless, creation of empty channels due to fibers decomposition and additional microcracks around the channels did not contribute significantly to the increase to the water permeability and UPV or decrease in mechanical properties, as presented by results of testing hereafter.

3.2. Residual properties of concrete

3.2.1. Mechanical properties

The results of mechanical testing (compressive strength and static

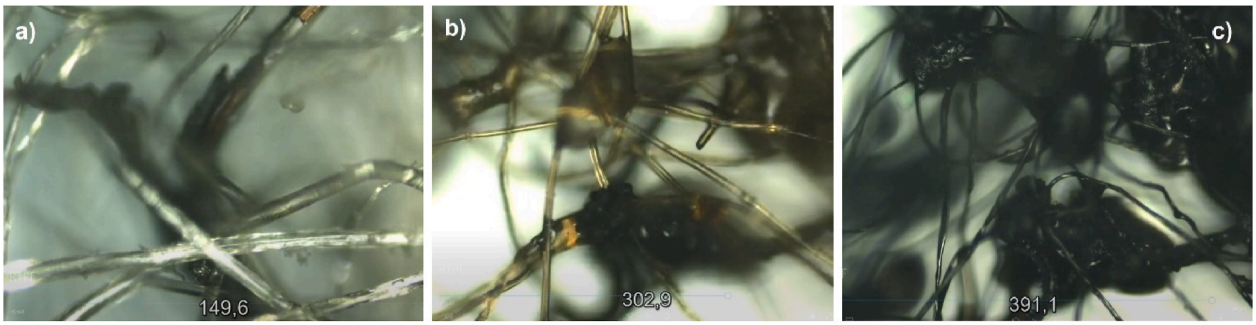

Fig. 8. a) Stable RTPF (image taken at 149.6 °C, b) RTPF melting and decreasing in volume (image taken at 302.9 °C and c) melted RTPF with leftover unburned residue (image taken at 391.1 °C).

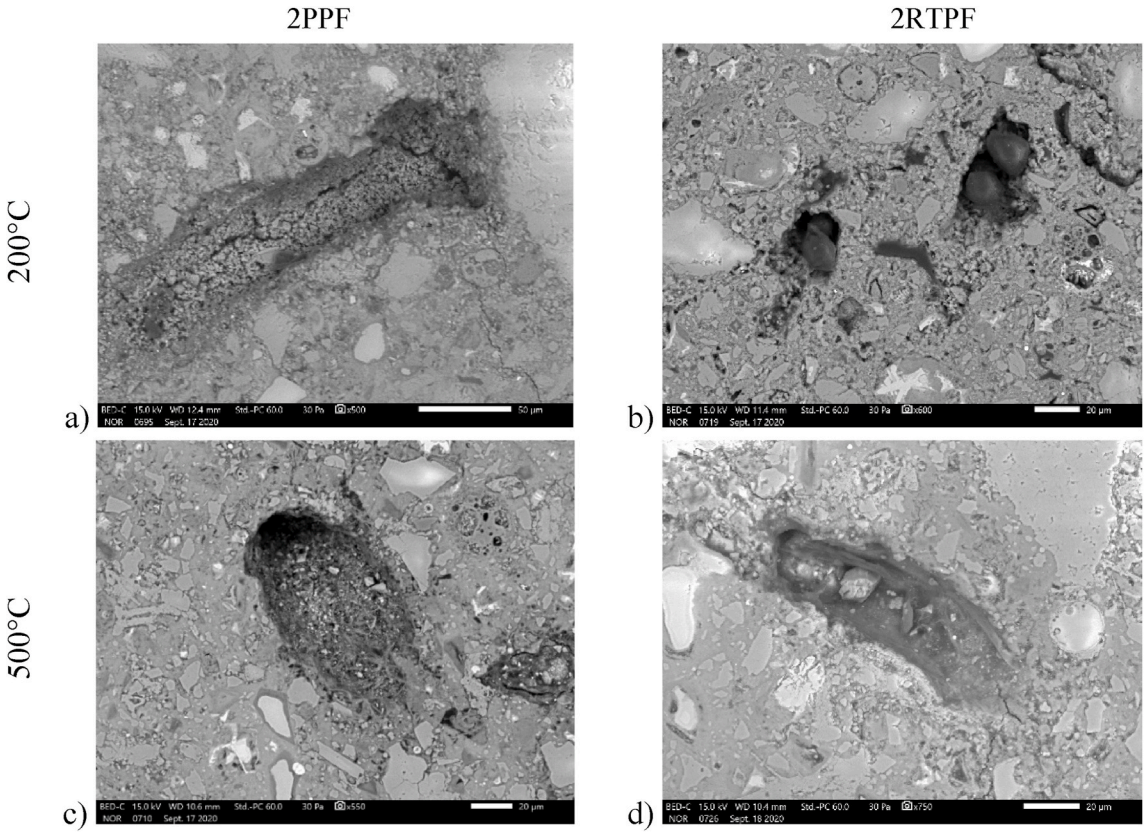

Fig. 9. SEM images before and after exposure to high temperatures for 2PPF and 2RTPF specimens.

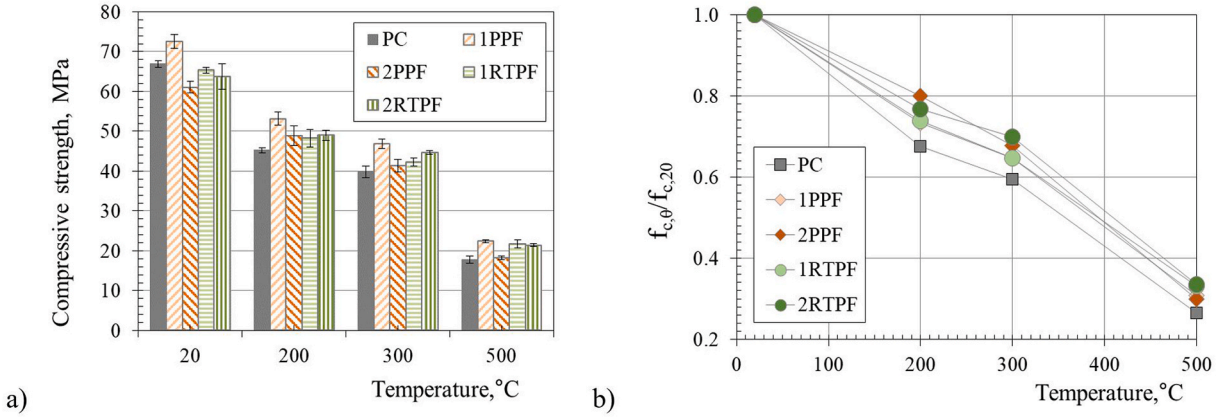

Fig. 10. Residual compressive strength vs temperature: a) mean and b) relative values.

modulus) are presented with average values and mean absolute deviations upon testing four specimens for compressive strength and three specimens for modulus of elasticity (Table B1 in the appendix B of the manuscript). Relative mechanical properties were calculated by dividing the residual property after particular temperature cycle ($f_{c,\theta}$, $E_{c,\theta}$, where $\theta = 200$, 300 and 500 °C) with initial ones ($f_{c,20}$, $E_{c,20}$).

Fig. 10a show the mean initial and residual compressive strengths of the tested mixes as a function of heating temperature (200, 300 and 500 °C). The initial compressive strength (referred to non-heated specimens) after one year ranged from 61.1 to 72.6 MPa. Compared to plain mix, the addition of 1 kg/m^3 PPF increased the compressive strength by 8.4%. On the contrary, all other tested mixes containing microfibers, i.e. 2PPF, 1RTPF and 2RTPF, had lower initial compressive strength by 8.7%, 2.4 and 4.7%, respectively.

Compared with the results of [53–55], the same trends can be observed for PPF mixes in this study. A positive effect on the compressive strength was obtained with the addition of 0.1% by volume of PPF fibres, while higher amounts caused its decrease. The increase in compressive strength with small amounts of fibres (up to 0.1%) is due to the ability of the uniformly distributed PPF fibres to bridge microcracks and prevent their further opening and coalescence into macrocracks.

Since the differences obtained between the tested mixes were within 10%, the results of the initial compressive strength are in good agreement with the studies presented in Refs. [34,56] which state that the addition of PPF and RTPF does not significantly affect the compressive strength, mainly due to the relatively low volume fraction of fibres in the concrete (0.22% in this case).

When the heating temperature increased from normal ambient conditions to a temperature of 500 °C, the mean compressive strength of all tested mixes decreased from 66.4 to 73.4% from the initial values. Compared to plain mix, the residual compressive strength was higher for all mixes with microfibers after heating from 200 to 500 °C.

Relative residual compressive strength as a function of temperature is presented in Fig. 10b showing very similar decreasing pattern for all tested mixes. Compared to the initial values, the compressive strength of the tested mixes decreased from 20% to 32.42% after heating to 200 °C, from 30% to 40% after 300 °C, and from 66.40% to 73.42% after 500 °C. As can be seen from Fig. 10b, mixes with microfibers (both PPF and RTPF) exhibited slightly higher (up to 12%) relative compressive strength compared to the plain mix after being exposed to all the target temperatures. Differences between mixes with PPF and RTPF are negligible.

The results obtained agree well with those of Behnood and Ghandehari [57] who concluded that the addition of PPF in an amount of 1–3 kg/m^3 increased the residual compressive strength of concretes after exposure to temperatures of 200–600 °C. This increase in compressive strength was explained by the reduction in thermal incompatibility between aggregates and cement pastes due to the melting and evaporation of PPF. Upon heating, aggregates (especially limestones as in this study) expand while cement pastes undergo thermal expansion up to about 150 °C and then shrinkage up to about 600–800 °C [1,2]. These incompatibility in thermal strain may affect the residual strength by forming stress concentrations in the concrete material. When the microfibers melt, they provide more free space and can act as shock absorbers that prevent severe deterioration of the concrete material. Opposed findings were obtained in studies [16,58,59], where decomposition of PPF cause a loss of compressive strength mainly due to the increased porosity in the concrete mix.

Fig. 11a and Table B.1 in the appendix B of the manuscript, show the mean residual static modulus of elasticity of the tested mixes as a function of heating temperature. The initial modulus of tested mixes after one year ranged from 39.74 to 44.52 GPa. Initial values of modulus of elasticity for tested mixes follow pattern obtained by compressive strength testing, i.e. compared to plain mix, the differences for mixes containing microfibers are lower than 10% (i.e. 8.4%) and the highest value was obtained within mix containing 1 kg/m^3 of PPF.

As the heating temperature increased from normal ambient conditions to a temperature of 500 °C, the mean modulus of all tested mixes decreased for more than 70%. Relative modulus of elasticity as a function of temperature was presented in Fig. 11b which show very similar behaviour for all tested mixes (differences lower than 6%). From the figure, it can be seen that after exposure to temperatures of 500 °C, differences between tested mixes almost diminished (in between 3.6%).

The reduction in the elastic modulus of concrete occurs due to the formation and development of cracks in heated concrete as a result of stresses within and between the concrete constituents (cement paste and aggregate), water vapour pressure, thermal stresses due to temperature differences between different parts of the concrete etc. From the results obtained, it can be generally concluded that the addition of fibres in relatively small volume fraction (up to 0.22% in this study), has no significant effect on the residual static modulus of elasticity. Results obtained for modulus of elasticity are further confirmed by UPV measurement presented in the next chapter of manuscript.

The results on the mechanical properties show that the addition of RTPF to the concrete in an amount up to 2 kg/m^3 does not cause any further degradation that could be caused by its melting and decomposition compared to a plain mix. Therefore, in the study on durability properties presented below, plain concrete and two concrete mixes with 2 kg/m^3 of PPF and RTPF, respectively, were considered.

3.2.2. *Durability properties*

As for mechanical properties, results obtained by durability testing (capillary absorption and UPV) are presented with average values upon testing three specimens (Table B.2 in the appendix B of manuscript and

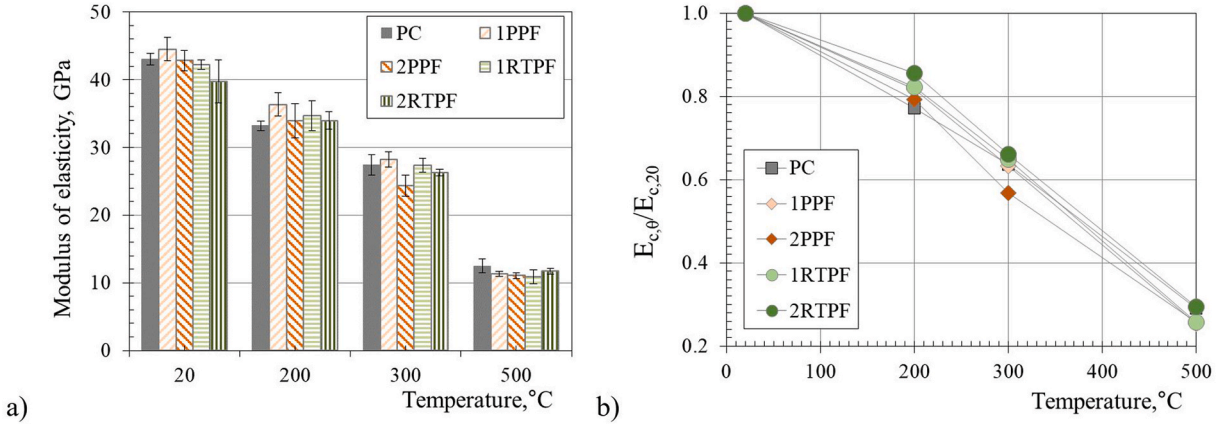

Fig. 11. Residual modulus of elasticity vs temperature: a) mean and b) relative values.

Figs. 12a and 14a. Relative values are presented in Figs. 12b and 14b.

Capillary absorption was observed over time as a function of weight gain. Fig. 12 presents results of measurement related to impact of three types of concrete (PC, 2PPF and 2RTPF) on the magnitude of capillary absorption changes as a result of different heating conditions. At room temperature and up to temperature of 300 °C, Fig. 12 a, b and c, slightly lower values were observed within mixes containing both types of fibres, which can be explained by pore blocking effect where fibers reduce connectivity of capillary pores. These results are in good agreement with those obtained in authors' previous study [33] while studied wet-sprayed concrete with addition of microfibers.

The results presented in Fig. 12d show that after exposure to 500 °C, the total amount of capillary pores was similar for all three mixes, but the capillary absorption coefficient (regarded as the initial slope of the curves) of the concrete with PPF was higher implying better connectivity of the capillary pores for 2PPF mix. Moreover, the increased water absorption for the 2PPF mix can be seen in Fig. 13, where an almost complete saturation of the specimens can be observed after only 1 h for these specimens. The DTA/TG analysis in Fig. 6 shows that both fiber types almost decompose at these temperatures. Although melting of the RTPF fibers might be expected to increase the capillary absorption coefficient after heating to 500 °C, probably due to the higher residue levels, as also shown by the DTA/TG analysis, the capillary absorption coefficient of the 2RTPF was comparable to that of plain concrete.

The results of capillary absorption are further confirmed by ultrasonic pulse velocity (UPV) test. A decrease in UPV may indicate cracks formation and an increase in porosity as a result of the effect of high temperature on concrete material [22]. Initial and residual UPV values after exposure to temperatures from 200 °C to 500 °C for tested concretes are presented in Fig. 14a. Initial values of UPV, which are higher and around 5 km/s indicating good initial quality of all tested mixes in accordance to Ref. [60]. Compared to plain mix, minor variations in UPV values (up to 3.2%) are to be noted with presence of microfibers.

As for other tested properties, the UPV values decreased up to 45% with the increased temperature to 500 °C. Relative UPV as a function of temperature was presented in Fig. 14b. Furthermore, in the entire observed temperature range, very similar results (the difference is lower than 5%). This observation lead to the conclusion that decomposition of microfibers (both PPF and RTPF) in low volumetric percentages (up to 0.22%) do not induce further increase in crack occurrence.

4. Conclusions

This study investigated the effect of recycled tyre polymer fibers (RTPF) on the residual mechanical and durability properties of concrete after high temperature exposure up to 500 °C taking into account fibres degradation temperatures determined by thermal analysis. The obtained results were compared with those of plain mix and mixes containing polypropylene fibres (PPF) which are usually used in concrete to mitigate explosive spalling in case of fire. Based on the experimental work and the analysis of the results, the following conclusions can be drawn:

– From the thermal analysis and comparison between PPF and RTPF, it can be concluded that PPF start melting at lower temperatures compared to RTPF, but their mass increases at first. PPF begin to lose their mass at 325 °C, with a peak in their decomposition at 450 °C. RTPF start melting at a temperature of 225 °C and immediately lose

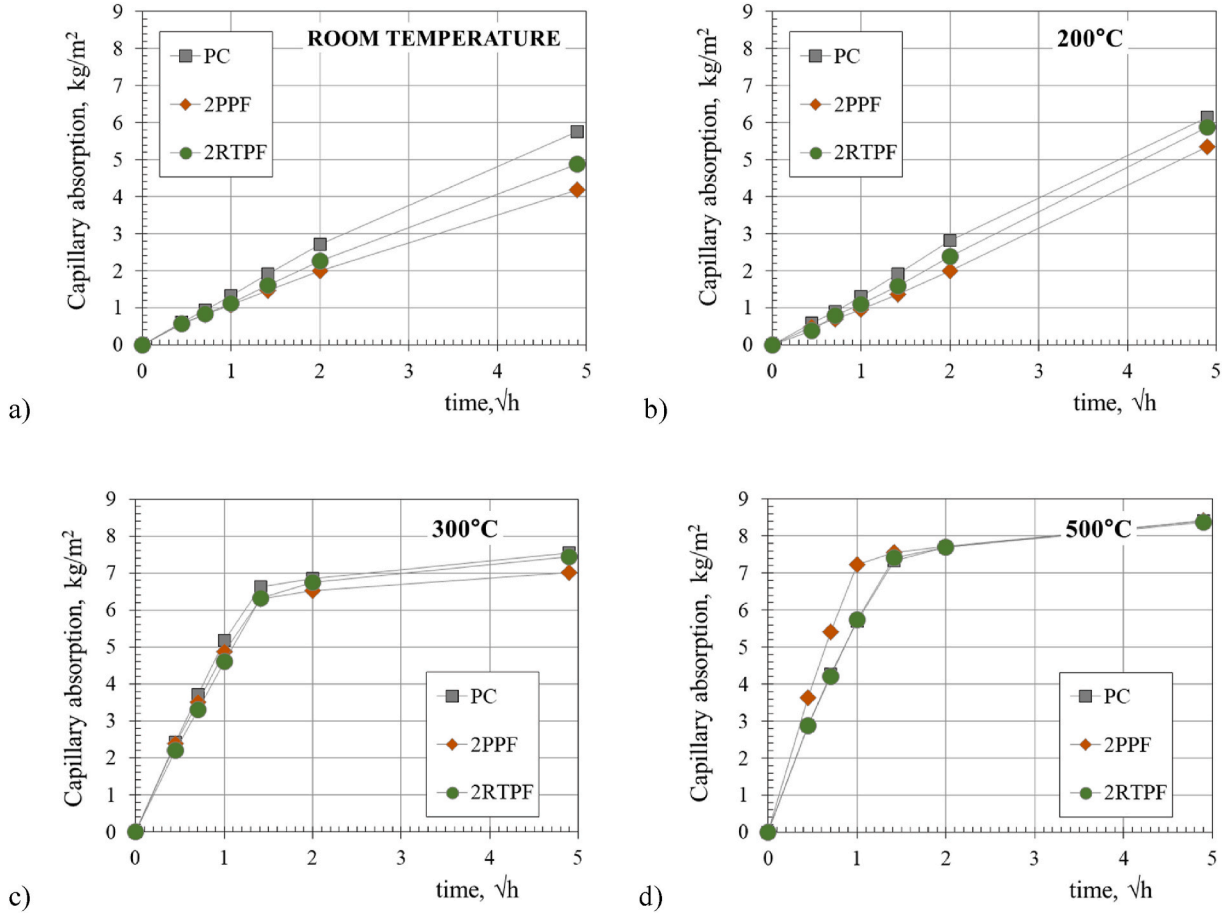

Fig. 12. Changes in capillary absorption of PC, 2PPF and 2RTPF concrete at a) room temperature and after exposure to temperatures b) 200 °C, c) 300 °C and d) 500 °C.

Fig. 13. Specimens heated to 500 °C for capillary absorption test at different time frames of testing.

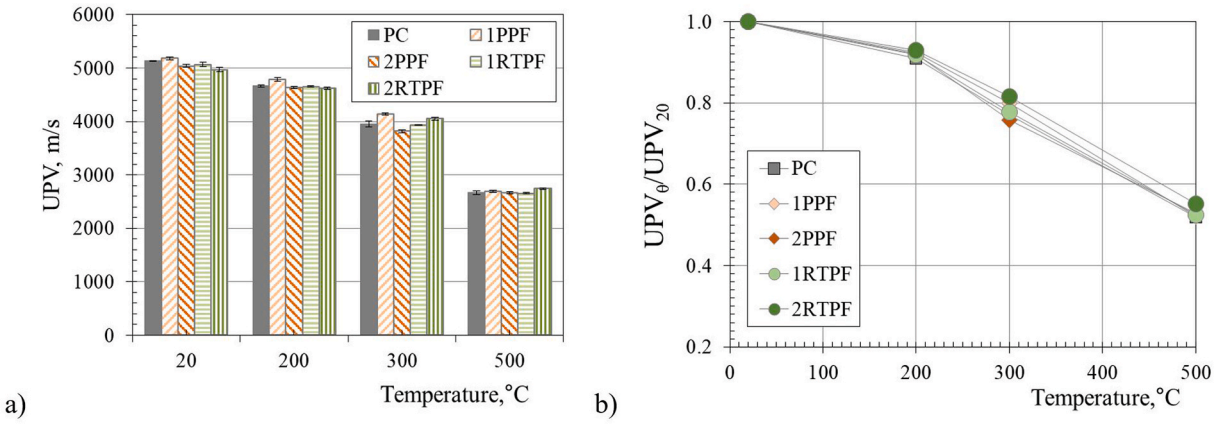

Fig. 14. Residual UPV of tested concrete a) mean and b) relative values.

mass, with a temperature peak at 395 °C. There is also a higher residual mass of unburned material (20% compared to 12% in PPF), which is due to unburned rubber bonded to RTPF.

– Degradation of both types of polymer fibres (PPF and RTPF) did not negatively affect the residual mechanical properties (compressive strength and modulus of elasticity). The residual compressive strength of all mixes containing fibers was slightly higher (up to 12%) compared to plain concrete mix, with mixes containing RTPF showing better behaviour. The same pattern was observed for

modulus of elasticity, but with smaller differences between the mixes.
- The addition of both polymer fibres to the concrete had a positive effect on capillary absorption up to a temperature of 300 °C. After heating to 500 °C, mix containing PPF had an increased water absorption compared to RTPF which can be explained by the higher amount of residues upon the melting.

Previous research has shown that RTPF can be used as a substitution to PPF to prevent explosive spalling in heated concrete. With this research it was further proven that this substitution will not induce negative effects on mechanical and durability properties of concrete. Even more, certain benefits of RTPF upon heating concrete to 500 °C were noticed, potentially attributed to the higher amount of residue compared to PPF. Considering the results of all the previous studies and the above experimental work with its conclusions, 2 kg/m^3 of cleaned RTPF can be prescribed as the optimum amount of fibres in concrete for fire aggressive environment.

Declaration of competing interest

The authors declare that they have no known competing financial interests or personal relationships that could have appeared to influence the work reported in this paper.

Acknowledgments

The studies presented in this paper are conducted within the project "Anagennisi: Innovative Reuse of all Tyre Components in Concrete" (grant no: 603722) funded by the European Commission under the 7th Framework Programme Environment topic. The first two authors also acknowledge the support of the project "Cementitious Composites Reinforced with Waste Fibres, ReWire (grant no. HRZZ-UIP-2020-02-5242), financed by Croatian Science Foundation. Authors would like to thank GUMIIMPEX for their support and students Petra Ružić and Krešimir Mesić for their contribution during experimental work.

Appendix A. Supplementary data

Supplementary data to this article can be found online at https://doi.org/10.1016/j.cemconcomp.2021.104184.

Appendix B. Results of mechanical and durability properties

Table B.1
Results of mechanical testing: mean values and mean absolute deviations

Temperature,°C/Mix	PC	1PPF	2PPF	1RTPF	2RTPF
Compressive strength, MPa					
non-heated	68.0 ± 0.83	72.6 ± 1.70	61.1 ± 1.51	65.3 ± 0.72	63.8 ± 3.21
200	45.3 ± 0.71	53.2 ± 1.69	48.9 ± 2.50	48.3 ± 2.23	49.0 ± 1.31
300	39.8 ± 1.47	46.9 ± 1.15	41.4 ± 1.59	42.3 ± 0.98	44.7 ± 0.44
500	17.8 ± 0.99	22.4 ± 0.36	18.3 ± 0.42	21.7 ± 1.03	21.4 ± 0.44
Modulus of elasticity, GPa					
non-heated	43.0 ± 1.21	44.5 ± 2.62	42.8 ± 2.33	42.2 ± 2.82	39.7 ± 1.53
200	33.2 ± 1.07	36.3 ± 1.07	33.9 ± 0.18	34.7 ± 0.84	34.0 ± 0.63
400	27.4 ± 1.29	28.2 ± 1.18	24.3 ± 0.61	27.4 ± 2.08	26.3 ± 0.72
600	12.5 ± 0.17	11.3 ± 0.26	11.1 ± 0.64	10.9 ± 0.52	11.7 ± 0.14

Table B.2
Results of durability testing: mean values and mean absolute deviations

Temperature, °C/Mix	PC	2PPF	2RTPF
Capillary absorption, %			
non-heated	4.8 ± 0.2	3.6 ± 0.6	4.5 ± 0.2
200	5.1 ± 0.2	4.6 ± 0.3	5.2 ± 0.0
300	6.3 ± 0.1	6.2 ± 0.1	6.4 ± 0.0
500	7.3 ± 0.0	7.5 ± 0.3	7.3 ± 0.1
Ultrasonic pulse velocity, km/s			
non-heated	5.13 ± 0.01	5.04 ± 0.03	4.97 ± 0.04
200	4.67 ± 0.02	4.63 ± 0.02	4.62 ± 0.02
300	3.95 ± 0.06	3.82 ± 0.0	4.05 ± 0.03
500	2.66 ± 0.03	2.66 ± 0.02	2.74 ± 0.02

References

[1] Z.P. Bazant, M.F. Kaplan, Concrete at High Temperatures: Materials Properties and Mathematical Models; State-Of-Art-Report, Longman Group Limited, 1996.
[2] G.A. Khoury, Y. Anderberg, K. Both, J. Fellinger, N.P. Hoj, C. Majorana, Fire Design of Concrete Structures – Materials, Structures and Modelling - State of Art Report, 2007.
[3] J. Bosnjak, Explosive Spalling and Permeability of High Performance Concrete under Fire – Numerical and Experimental Investigations, 2014. Stuttgart.
[4] I. Hager, K. Mróz, Role of polypropylene fibres in concrete spalling risk mitigation in fire and test methods of fibres effectiveness evaluation, Materials 12 (2019) 3869, https://doi.org/10.3390/ma12233869.
[5] T.G.V. van der Waart van Gulik, A.J. Breunese, R. Jansson, L. Boström, E. Annerel, Spalling behaviour of a non-spalling qualified concrete, in: F. Dehn (Ed.), 4th Int. Work. Concr. Spalling Due to Fire Expo, MFPA Leipzig GmbH, 2015, pp. 2017–2227.
[6] M. Ozawa, H. Morimoto, Effects of various fibres on high-temperature spalling in high-performance concrete, Construct. Build. Mater. 71 (2014) 83–92, https://doi.org/10.1016/j.conbuildmat.2014.07.068.

[7] L.T. Phan, Pore pressure and explosive spalling in concrete, Mater. Struct. Constr. 41 (2008) 1623–1632, https://doi.org/10.1617/s11527-008-9353-2.

[8] M.B. Dwaikat, V.K.R. Kodur, Hydrothermal model for predicting fire-induced spalling in concrete structural systems, Fire Saf. J. 44 (2009) 425–434, https://doi.org/10.1016/j.firesaf.2008.09.001.

[9] P. Kalifa, G. Chéné, C. Gallé, High-temperature behaviour of HPC with polypropylene fibres, Cement Concr. Res. 31 (2001) 1487–1499, https://doi.org/10.1016/s0008-8846(01)00596-8.

[10] J. Zhao, J.J. Zheng, G.F. Peng, K. Van Breugel, A meso-level investigation into the explosive spalling mechanism of high-performance concrete under fire exposure, Cement Concr. Res. 65 (2014) 64–75, https://doi.org/10.1016/j.cemconres.2014.07.010.

[11] H.L. Zhang, C.T. Davie, A numerical investigation of the influence of pore pressures and thermally induced stresses for spalling of concrete exposed to elevated temperatures, Fire Saf. J. 59 (2013) 102–110, https://doi.org/10.1016/j.firesaf.2013.03.019.

[12] Y. Fu, L. Li, Study on mechanism of thermal spalling in concrete exposed to elevated temperatures, Mater. Struct. Constr. 44 (2011) 361–376, https://doi.org/10.1617/s11527-010-9632-6.

[13] J.-C. Liu, K.H. Tan, Y. Yao, A new perspective on nature of fire-induced spalling in concrete, Construct. Build. Mater. 184 (2018) 581–590, https://doi.org/10.1016/j.conbuildmat.2018.06.204.

[14] G.A. Khoury, B. Willoughby, Polypropylene fibres in heated concrete. Part 1: molecular structure and materials behaviour, Mag. Concr. Res. 60 (2008) 125–136, https://doi.org/10.1680/macr.2008.60.2.125.

[15] G.A. Khoury, Polypropylene fibres in heated concrete. Part 2: pressure relief mechanisms and modelling criteria, Mag. Concr. Res. 60 (2008) 189–204, https://doi.org/10.1680/macr.2007.00042.

[16] M. Zeiml, D. Leithner, R. Lackner, H.A. Mang, How do polypropylene fibers improve the spalling behavior of in-situ concrete? Cement Concr. Res. 36 (2006) 929–942, https://doi.org/10.1016/j.cemconres.2005.12.018.

[17] R. Jansson, L. Boström, The influence of pressure in the pore system on fire spalling of concrete, Fire Technol. 46 (2010) 217–230, https://doi.org/10.1007/s10694-009-0093-9.

[18] HZN Standards Publication, HRN EN 1992-1-2 Eurocode 2: Design of Concrete Structures – Part 1-2: General Rules – Structural Fire Design (EN 1992-1-2:2004+AC:2008), Croatian Standards Institute, Zagreb, Croatia, 2008.

[19] D. Zhang, K.H. Tan, Critical Fibre Dimensions for Preventing Spalling of Ultra, Proc. 11th Int. Conf. Struct. Fire, 2020, pp. 333–341.

[20] A. Bilodeau, V.K.R. Kodur, G.C. Hoff, Optimization of the type and amount of polypropylene fibres for preventing the spalling of lightweight concrete subjected to hydrocarbon fire, Cement Concr. Compos. 26 (2004) 163–174, https://doi.org/10.1016/S0958-9465(03)00085-4.

[21] J. Bošnjak, J. Ožbolt, R. Hahn, Permeability measurement on high strength concrete without and with polypropylene fibers at elevated temperatures using a new test setup, Cement Concr. Res. 53 (2013) 104–111, https://doi.org/10.1016/j.cemconres.2013.06.005.

[22] J. Albrektsson, Durability of Fire Exposed Concrete, KTH Royal Institute of Technology, 2015.

[23] K. Pistol, F. Weise, B. Meng, U. Schneider, The mode of action of polypropylene fibres in high performance concrete at high temperatures, in: 2nd Int. RILEM Work. Concr. Spalling Due to Fire Expo, 2011, pp. 289–296.

[24] J. Bošnjak, A. Sharma, Mechanical properties of concrete with steel and polypropylene fibres at elevated temperatures, Fibers 7 (2019), https://doi.org/10.3390/FIB7020009.

[25] N. Banthia, R. Gupta, Influence of polypropylene fiber geometry on plastic shrinkage cracking in concrete, Cement Concr. Res. 36 (2006) 1263–1267, https://doi.org/10.1016/j.cemconres.2006.01.010.

[26] I.M.G. Bertelsen, L.M. Ottosen, G. Fischer, Influence of fibre characteristics on plastic shrinkage cracking in cement-based materials: a review, Construct. Build. Mater. 230 (2020), https://doi.org/10.1016/j.conbuildmat.2019.116769.

[27] G. Olivier, R. Combrinck, M. Kayondo, W.P. Boshoff, Combined effect of nano-silica, super absorbent polymers, and synthetic fibres on plastic shrinkage cracking in concrete, Construct. Build. Mater. 192 (2018) 85–98, https://doi.org/10.1016/j.conbuildmat.2018.10.102.

[28] D. Saje, B. Bandelj, J. Šušteršić, Shrinkage of polypropylene fiber-reinforced high-performance concrete, J. Mater. Civ. Eng. 23 (2010) 941–953, https://doi.org/10.1061/(ASCE)MT.1943-5533.0000258.

[29] C.K.Y. Leung, R. Lai, A.Y.F. Lee, Properties of wet-mixed fiber reinforced shotcrete and fiber reinforced concrete with similar composition, Cement Concr. Res. 35 (2005) 788–795, https://doi.org/10.1016/j.cemconres.2004.05.033.

[30] A.A. Ramezanianpour, M. Esmaeili, S.A. Ghahari, M.H. Najafi, Laboratory study on the effect of polypropylene fiber on durability, and physical and mechanical characteristic of concrete for application in sleepers, Construct. Build. Mater. 44 (2013) 411–418, https://doi.org/10.1016/j.conbuildmat.2013.02.076.

[31] P. Zhang, Q.F. Li, Effect of polypropylene fiber on durability of concrete composite containing fly ash and silica fume, Compos. B Eng. 45 (2013) 1587–1594, https://doi.org/10.1016/j.compositesb.2012.10.006.

[32] I. Netinger Grubeša, B. Marković, A. Gojević, J. Brdarić, Effect of hemp fibers on fire resistance of concrete, Construct. Build. Mater. 184 (2018) 473–484, https://doi.org/10.1016/j.conbuildmat.2018.07.014.

[33] A. Baricevic, M. Pezer, M. Jelcic Rukavina, M. Serdar, N. Stirmer, Effect of polymer fibers recycled from waste tires on properties of wet-sprayed concrete, Construct. Build. Mater. 176 (2018) 135–144, https://doi.org/10.1016/j.conbuildmat.2018.04.229.

[34] A. Baričević, M. Jelčić Rukavina, M. Pezer, N. Štirmer, Influence of recycled tire polymer fibers on concrete properties, Cement Concr. Compos. 91 (2018) 29–41, https://doi.org/10.1016/j.cemconcomp.2018.04.009.

[35] M. Serdar, A. Baričević, M. Jelčić Rukavina, M. Pezer, D. Bjegović, N. Štirmer, Shrinkage behaviour of fibre reinforced concrete with recycled tyre polymer fibres, Int. J. Polym. Sci. 2015 (2015), https://doi.org/10.1155/2015/145918.

[36] M. Grubor, N. Štirmer, M.J. Rukavina, A. Baričević, Effect of recycled tire polymer fibers on autogenous deformation of self-compacting concrete, RILEM Tech. Lett. 5 (2020) 33–40, https://doi.org/10.21809/rilemtechlett.2020.115.

[37] Martina Grubor, Volume Deformations of Cement Composites with Recycled Tyre Polymer Fibers, PhD thesis, University of Zagreb Faculty of civil engineering, Zagreb, 2020.

[38] O. Onuaguluchi, N. Banthia, Durability performance of polymeric scrap tire fibers and its reinforced cement mortar, Mater. Struct. Constr. 50 (2017), https://doi.org/10.1617/s11527-017-1025-7.

[39] M. Chen, H. Zhong, M. Zhang, Flexural fatigue behaviour of recycled tyre polymer fibre reinforced concrete, Cement Concr. Compos. 105 (2020), https://doi.org/10.1016/j.cemconcomp.2019.103441.

[40] G.M. Chen, C.J. Lin, H. Yang, Y.H. He, H.Z. Zhang, J.F. Chen, Fracture behaviour of steel fibre reinforced recycled aggregate concrete after exposure to elevated temperatures, Construct. Build. Mater. 128 (2016) 272–286, https://doi.org/10.1016/j.conbuildmat.2016.10.072.

[41] F.P. Figueiredo, S.S. Huang, H. Angelakopoulos, K. Pilakoutas, I. Burgess, Effects of Recycled Steel and Polymer Fibres on Explosive Fire Spalling of Concrete, Fire Technol, 2019, https://doi.org/10.1007/s10694-019-00817-9.

[42] F.P. Figueiredo, A.H. Shah, S.S. Huang, H. Angelakopoulos, K. Pilakoutas, I. Burgess, Fire protection of concrete tunnel linings with waste tyre fibres, Procedia Eng 210 (2017) 472–478, https://doi.org/10.1016/j.proeng.2017.11.103.

[43] F. Figueiredo, I. Rickard, A.H. Shah, S.-S. Huang, H. Angelakopoulos, L.A. Bisby, I. Burgess, K. Pilakoutas, Recycled tyre polymer fibres to mitigate heat-induced spalling of concrete, Proc. from 5th Int. Work. Concr. Spalling. (2017) 359–364.

[44] C.C. Santos, J.P.C. Rodrigues, Compressive strength at high temperatures of a concrete made with recycled tire textile and steel fibers, MATEC Web Conf 6 (2013), https://doi.org/10.1051/matecconf/20130607004.

[45] HZN Standards Publication, Tests for geometrical properties of aggregates - Part 4: determination of particle shape - shape index; HRN EN, Croatian Standards Institute, Zagreb, Croatia, 2008.

[46] HZN Standards Publication, HRN EN 197-1 Cement - Part 1: Composition Specifications and Conformity Criteria for Comon Cements, Croatian Standards Institute, Zagreb, Croatia, 2012.

[47] RILEM Technical Committee, Recommendation of RILEM TC 200-HTC, Mechanical concrete properties at high temperatures—modelling and application, Part 1: introduction - General presentation, Mater. Struct. 40 (2007) 841–853, https://doi.org/10.1617/s11527-006-9203-z.

[48] RILEM TC 129 MHT, Test methods for mechanical properties of concrete at high temperatures - compressive strength for service and accident conditions, Mater. Struct. 28 (1995) 410–414, https://doi.org/10.1007/BF02473077.

[49] RILEM TC 129-MHT, Test methods for mechanical properties of concrete at high temperatures - modulus of elasticity for service and accident conditions, Mater. Struct. 37 (2004) 139–144. https://doi.org/10.1007/BF02486610.

[50] K.D. Hertz, Concrete strength for fire safety design, Mag. Concr. Res. 57 (2005) 445–453, https://doi.org/10.1680/macr.2005.57.8.445.

[51] HZN Standards Publication, HRN EN 13057 Products and Systems for the Protection and Repair of Concrete Structures -- Test Methods -- Determination of Resistance of Capillary Absorption, Croatian Standards Institute, Zagreb, Croatia, 2003.

[52] HZN Standards Publication, HRN EN 12504-4 Testing Concrete -- Part 4: Determination of Ultrasonic Pulse Velocity, Croatian Standards Institute, Zagreb, Croatia, 2004.

[53] Z. Bayasi, J. Zeng, Properties of polypropylene fiber reinforced concrete, ACI Mater. J. (1993) 605–610.

[54] A. Sadrmomtazi, A. Fasihi, Influence of polypropilene fibers on the performance of nano--incorporated mortar, Iran, J. Sci. Technol. Trans. B. 34 (2010) 385–395.

[55] P.S. Song, S. Hwang, B.C. Sheu, Strength properties of nylon- and polypropylene-fiber-reinforced concretes, Cement Concr. Res. 35 (2005) 1546–1550, https://doi.org/10.1016/j.cemconres.2004.06.033.

[56] S. Zhang, B. Zhao, Influence of polypropylene fibre on the mechanical performance and durability of concrete materials, Eur. J. Environ. Civ. Eng. 16 (2012) 1269–1277, https://doi.org/10.1080/19648189.2012.709681.

[57] A. Behnood, M. Ghandehari, Comparison of compressive and splitting tensile strength of high-strength concrete with and without polypropylene fibers heated to high temperatures, Fire Saf. J. 44 (2009) 1015–1022, https://doi.org/10.1016/j.firesaf.2009.07.001.

[58] P. Pliya, A.L. Beaucour, A. Noumowé, Contribution of cocktail of polypropylene and steel fibres in improving the behaviour of high strength concrete subjected to high temperature, Construct. Build. Mater. 25 (2011) 1926–1934, https://doi.org/10.1016/j.conbuildmat.2010.11.064.

[59] S.L. Suhaendi, T. Horiguchi, Effect of short fibers on residual permeability and mechanical properties of hybrid fibre reinforced high strength concrete after heat exposition, Cement Concr. Res. 36 (2006) 1672–1678, https://doi.org/10.1016/j.cemconres.2006.05.006.

[60] A. Neville, Properties of Concrete, fourth ed., Longman Group Limited, 1995.